# Dispersing Individual Single-Wall Carbon Nanotubes in Aqueous Surfactant Solutions below the cmc

**Cite as:**
**Angelikopoulos, P., Gromov, A., Leen, A., Nerushev, O., Bock, H., & Campbell, E. E. B. (2010). Dispersing Individual Single-Wall Carbon Nanotubes in Aqueous Surfactant Solutions below the CMC. *Journal of Physical Chemistry C*, 114(1), 29.**

**Manuscript received: 24/06/2009; Revised: 22/09/2009; Article published: 11/12/2009**

# Dispersing Individual Single-Wall Carbon Nanotubes in Aqueous Surfactant Solutions Below the CMC**

Panagiotis Angelikopoulos,[1] Andrei Gromov,[2,*] Ailsa Leen,[2,3] Oleg Nerushev,[2] Henry Bock[1,*] and Eleanor E.B Campbell[2,4]

[1]Department of Chemical Engineering, Heriot-Watt University, Edinburgh, EH14 4AS, UK.

[2]EaStCHEM, School of Chemistry, Joseph Black Building, University of Edinburgh, West Mains Road, Edinburgh, EH9 3JJ, UK.

[3]Mary Erskine School, Edinburgh EH4 3NT, UK.

[4]Department of Physics, Konkuk University, Seoul 143-701, Korea.

[*]Corresponding authors; H.B. e-mail: h.bock@hw.ac.uk; A.G. e-mail: a.v.gromov@ed.ac.uk

[**]Financial support for an EPSRC DTA award and from EastChem is gratefully acknowledged. A.L. acknowledges financial support from the Nuffield Foundation.

**Graphical abstract:**

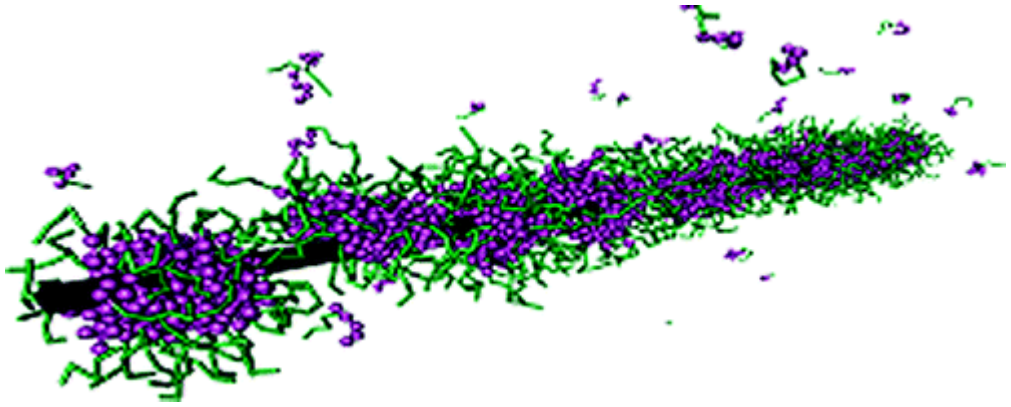

**Abstract**

Dispersions of single wall carbon nanotubes (SWCNTs) in surfactant solutions below the critical micelle concentration (CMC) have been studied theoretically and experimentally. Dissipative Particle Dynamics (DPD) simulations of a coarse-grained model predicts that surfactant adsorption on small diameter tubes is dominated by aggregation of the surfactant molecules into adsorbed micelles at $C \approx 0.3\ C_{CMC}$. We also find that the surfactant adsorption is nearly complete at a concentration of around $C \approx 0.5\ C_{CMC}$. Further increase of the surfactant concentration has only minor effects on the radial density of surfactant headgroups, indicating that SWCNT may be fully stabilized in solutions below the CMC. SWCNT dispersions in solutions of anionic surfactants sodium dodecyl sulphate (SDS) and sodium dodecylbenzenesulphonate (SDBS) below the CMC show a significant fraction of dispersed individual tubes and small bundles, in agreement with the model calculations.

**Introduction**

Preparation of high concentration stable dispersions of debundled carbon nanotubes (CNTs) is an important challenge for a number of current and potential applications of CNTs, e.g. mechanical reinforcement of polymer[1,2] and metal[3] matrices, development of conducting polymeric materials[4-6], improvement of thermal conductivity of composites[7-12] etc. Also, dispersion of individual nanotubes is indispensable for separation of SWCNT according to their electronic properties[13-18].

However, due to strong van der Waals forces, carbon nanotubes tend to form bundles. The general approach for producing dispersions of unbundled non-functionalized CNTs includes splitting bundles by input of energy (e.g. ultrasonication) in the presence of a stabilizing agent which would prevent reagglomeration of the CNTs into bundles. Different classes of stabilizing agents have been used such as (i) aqueous solutions of numerous surfactants[19-24]; (ii) solutions of synthetic[25-30] and bio-polymers[31-37] in appropriate solvents (in this case stabilization of CNTs in solution proceeds due to polymer wrapping around the tube along its axis); (iii) ionic liquids and solutions of organic salts[38-40]. Recently it was also shown that a significant degree of dispersion can be achieved by spontaneous debundling in common organic solvents such as N-methyl-2-pyrrolidone[41] and γ-butyrolactone[42]. Covalent functionalisation also may be used to facilitate the dispersion of CNTs[43-50]. It must, however, be taken into account that sidewall functionalisation of SWCNT changes their properties[51-57].

For preparation of stable dispersions with relatively high concentrations of CNTs it is generally recommended in the literature to use surfactant concentrations equal to several critical micelle concentration (CMC) values [22,23,58-61]. Even at the optimum concentration of surfactants, dispersions with a large fraction of individual SWCNT have only been reported for low concentrations of SWCNT. There are only a few publications where

CNT dispersions in surfactant solutions with concentrations close to or below CMC were reported [59,60,62,63], although, without much emphasis on the properties of such dispersions .

Whether surfactant adsorption on CNTs leads to their dispersion or not, clearly depends on the adsorbed amount and possibly also on the adsorbed structures. Both are difficult to access experimentally but are available through computer simulations. This potential of molecular simulations is demonstrated by a number of recent studies: In their Coarse Grained Molecular Dynamics (CGMD) simulations Shvartzman-Cohen et al.[64] found that amphiphilic block-copolymers of the Pluronic family form adsorbed random structures on CNTs. Wallace et al.[65,66] used CGMD to investigate adsorption of DPPC (dipalmitoyl phosphatidylcholine) and DHPC (dihexanoyl phosphatidylcholine) phospholipids and zwitterionic detergent LPC (lysophosphatidylcholine) on CNTs. They found a variety of adsorbed structures including randomly arranged surfactant molecules and encapsulation by spherical and cylindrical micelles, which depend on the type of amphiphile as well as the number of surfactant molecules in the simulation box. Tummala et al.[67] used fully atomistic MD to show that the aggregation morphology of Na-dodecyl sulphate (SDS) molecules on SWCNTs is influenced by the tube diameter, its chirality and by the number of SDS molecules placed in the simulation box. Specifically, they find an increase in the adsorbed amount and variation from "rings" of SDS molecules lying flat on the tube surfaces and parallel to the tube axis to adsorbed micelles with disordered internal structure when the number of surfactants in the simulation box was increased.

Patel et al.[68] studied the dispersion of two parallel nanotubes with the surfactant DTMAC (n-decyltrimethylammonium chloride) using 2D Density Functional Theory and a coarse grained model with implicit solvent. Their results indicate that SWCNT dispersions may occur below the CMC, since the surfactant mediated force overcomes the direct SWCNT-SWCNT attraction. This conclusion was drawn by studying the system below the experimental CMC, thus, not taking into account likely deviations of the model CMC compared to the bulk CMC.

While these studies demonstrate a dependence of the adsorbed amount and the adsorbed structures on the number of molecules in the simulation box, concentration control has not been achieved. Consequently, knowledge and understanding of the concentration dependence of surfactant adsorption on CNTs is still lacking. This, however, is essential for the interpretation of experimental findings as well as the optimization of technical processes and applications.

Here we report on the preparation of stable aqueous dispersions with increased fraction of individual SWCNT in anionic surfactant solutions below the CMC. In the simulation part of this manuscript we use dissipative particle dynamics (DPD) and a coarse-grained surfactant model to investigate the concentration dependence of surfactant adsorption on CNTs. Specifically we study the adsorbed amount and the adsorbed structures. Using the bulk CMC as a reference we find good agreement between the experimental and the simulation results. In particular, the dispersion of CNTs below the CMC is demonstrated and explained.

## Experimental and Simulation Methods

### *Experiments*

Typically 1 mg of SWCNTs (as produced HiPco[69] tubes from Carbon Nanotechnologies Inc., USA) was dispersed in 10 ml of surfactant solution (concentration of SWCNTs, $c_{CNT}$ - 0.1mg/ml). The following surfactant solutions were used (see Table 2): SDS (Na dodecyl sulphate, $CMC_{SDS}$ value in water is 2.4 mg/ml [70,71]): 10 mg/ml, ~4 CMC (further denoted as SDS10); 3 mg/ml, ~1.2 CMC (further denoted as SDS3); 1 mg/ml, ~0.4 CMC (further denoted as SDS1); and 0.5 mg/ml, ~0.2 CMC (further denoted as SDS05);

SDBS (Na dodecylbenzenesulphonate, $CMC_{SDBS}$ value in water is 0.35 mg/ml [60]): 10 mg/ml, ~30 CMC (further denoted as SDBS10); 3 mg/ml, 8-9 CMC further denoted as (SDBS3), 1 mg/ml, ~3 CMC (further denoted as SDBS1) and 0.2 mg/ml, ~0.6 CMC (further denoted as SDBS 02).

The dispersions were sonicated with an ultrasonic tip (*Bandelin Sonoplus* Ultrasonic homogenizer HD 2200 with titanium tip KE76 with a diameter of 6 mm) in plastic test-tubes at an average power of 20W for 6-7 min (in 1 min periods in order not to overheat the sample) while cooling in an ice bath. Subsequently the dispersions were centrifuged for 2 x 30min at 20500g. The supernatant fraction of each dispersion was analyzed by AFM. As there was always some precipitant visible, the actual concentrations of SWCNTs in the supernatant were always lower than the original 0.1 mg/ml.

AFM measurements were performed using a Veeco DI *NanoMan* VS instrument in tapping mode. For preparation of samples for AFM a piece of polished Si wafer, surface modified with (3-aminopropyl)triethoxysilane for better adhesion of SWCNT[72-74], was completely covered with the supernatant part of the SWCNT dispersion and left for 3 h in saturated water vapour environment for prevention of liquid evaporation . Then the substrate was rinsed in distilled water and blown dry with nitrogen gas.

The concentrations of SWCNT in the original dispersions and the dispersions after centrifugation were evaluated by Raman spectroscopy. A Renishaw InVia Raman confocal microscope with an excitation energy of 2.41 eV was used for the Raman studies. The dispersions were analysed through a 90 μm thick glass slide using backscattering geometry and a laser power of 3 mW.

### *Simulations*

#### Model

The simulation method and the model employed in this study have been used and discussed in detail before[75] therefore we confine this section to a brief overview. The surfactant molecules used in this study ($H_5T_5$) are represented as chains of five hydrophilic head (*H*) beads followed by five hydrophobic tail (*T*) beads. The

solvent is treated implicitly. The beads interact via effective potentials due to the coarse-grained character of the surfactant beads along with the implicit representation of the solvent. In this study we employ a common empirical model where the interaction between hydrophobic beads is attractive, while all other bead/bead interactions are repulsive. The force shifted Lennard-Jones (LJ) (12,6) potential $\phi_{ij}$ is used to represent attractive interactions between beads i and j:

$$\phi(r_{ij}) = \begin{cases} \phi_{\mathrm{LJ}(r_{ij})} + \phi'_{\mathrm{LJ}}(r_{\mathrm{cut}})(r_{ij} - r_c) - \phi_{\mathrm{LJ}}(r_{\mathrm{cut}}) & r_{ij} < r_{\mathrm{cut}} \\ 0 & r_{ij} \geq r_{\mathrm{cut}} \end{cases} \qquad (1)$$

$$\phi_{\mathrm{LJ}(r_{ij})} = 4\varepsilon\left[\left(\frac{\sigma}{r_{ij}}\right)^{12} - \left(\frac{\sigma}{r_{ij}}\right)^{6}\right]$$

where $\phi'_{LJ}(r) = d\phi_{LJ}/dr$ and $r_{cut}$ is the cut-off-radius. In eq (1) $\varepsilon$ and $\sigma$ are the well depth and the length parameter of the LJ potential, respectively, $r_{ij} = \|\boldsymbol{r}_{ij}\|$, $\boldsymbol{r}_{ij} = \boldsymbol{r}_j - \boldsymbol{r}_i$ and $\boldsymbol{r}_i$ and $\boldsymbol{r}_j$ are the positions of beads i and j, respectively. Repulsive interactions are modelled using the WCA potential given by eq (1) with $r_{cut} = \sqrt[6]{2}$. Beads k and l which are nearest neighbours in a chain interact via the bead/bead potentials and, additionally, via a quadratic harmonic bond potential

$$\phi_{bond}(r_{kl}) = \varepsilon_{bond}(r_{kl} - \sigma_{bond})^2, \qquad (2)$$

where $\varepsilon_{bond}$ and $\sigma_{bond}$ are the well depth and the bond length, respectively.

At the level of coarse graining of the surfactant molecules, CNTs can be regarded as smooth cylinders. Their interactions with surfactant beads are modelled via the force shifted Lennard-Jones (12,6) potential in eq (1) which is also shifted to the surface of the nanotubes

$$\phi_{CNT}(r_i) = \varepsilon_{CNT}\phi(r_i - r_{CNT}), \qquad (3)$$

where $r_i$ is the shortest distance[76] between bead i and the nanotube axis and $r_{CNT}$ is the radius of the nanotube. All simulation parameters are summarized in Table 1.

***Table 1.*** Simulation parameters in reduced units.

| Surfactants | |
|---|---|
| number of T-beads = 5 | number of H-beads = 5 |
| $\varepsilon = 1.0$ | $\sigma = 1.0$ |
| attractive: $r_{cut}=2.5$ | repulsive: $r_{cut}=\sqrt[6]{2}$ |
| $\varepsilon_{bond} = 4.0$ | $\sigma_{bond} = 1.2$ |
| Nanotubes | |
| $r_{CNT} = 1.0$ | $\varepsilon_{CNT} = 2.5$ |
| Simulation | |
| T=0.7 | $\Delta t=0.005$ |
| non-conservative: $r_{cut}=2.5$ | $\xi=1$ |
| equilibration=$10^8\Delta t$ | production=$10^8\Delta t$ |

***Table 2.*** Parameters of SWCNT dispersions.

| Dispersion | Surfactant concentration (mg/ml) | Surfactant concentration in CMC | SWCNT concentration (mg/ml) in supernatant | Surfactant -to-SWCNT ratio (w/w) | $D_{rms}$ ($\sqrt{<D^2>}$) (nm) | Fraction of individual tubes, %** | Maximal value of diameter observed in supernatant, (nm) |
|---|---|---|---|---|---|---|---|
| SDBS10 | 10 | 26.61 | 0.0325 | 307.7 | 1.818 | 35 | 4.3 |
| SDBS3 | 3 | 7.98 | 0.032 | 93.8 | 2.051 | 22 | 4.4 |
| SDBS1 | 1 | 2.66 | 0.0265 | 37.7 | 1.714 | 47 | 4.5 |
| SDBS02 | 0.2 | 0.53 | 0.0095 | 21.1 | 1.250 | 67 | 2.7 |
| | | | | | | | |
| SDS10 | 10 | 4.34 | 0.0305 | 327.9 | 1.503 | 52 | 3.3 |
| SDS3 | 3 | 1.3 | 0.0225 | 133.3 | 2.105 | 32 | 4.9 |
| SDS1 | 1 | 0.43 | 0.0105 | 95.2 | 1.342 | 63 | 2.8 |
| SDS05 | 0.5 | 0.22 | 0.0032 | 156.3* | 0.815 | 98 | 1.5 |

* - this is an overevaluated number since it does not take into account the consumption of surfactant on air-liquid and liquid-solid (walls of the container) interfaces

** - assuming that species with diameter < 1.3nm are individual tubes

**Simulation Methodology**

We investigate the system in the canonical ensemble using the dissipative particle dynamics (DPD) method[77]. In DPD any two particles i and j interact via a pair wise force $\boldsymbol{F}_{ij}=\boldsymbol{F}_{ij}^{C}+\boldsymbol{F}_{ij}^{R}+\boldsymbol{F}_{ij}^{D}$ where $F_{ij}^{C}$, $F_{ij}^{R}$ and $F_{ij}^{D}$ are the conservative, the random and the dissipative force, respectively. The conservative force is given by the derivative of the potentials discussed above. As the random and dissipative forces should not affect the equilibrium results we chose them to be the same as the ones commonly used in most studies (e.g. [75,78]).

The simulation box is large which allows us to determine and control the bulk surfactant concentration (Figure 1). To determine the bulk concentration, a slice of the system of 50σ width centred at the tube axis in the x-direction (perpendicular to the tube axis) was excluded. The remaining volume is considered bulk-like. The size of the simulation box was chosen such that there were typically 200 chains in the bulk control volume but no less than 40 in uncritical cases and no less than 160 chains adsorbed. The concentration is adjusted in the initial part of the equilibration period by insertion and deletion of surfactant molecules if the actual concentration in the bulk-like region deviates by more than 5% from the target. The usual periodic boundary conditions are also employed.

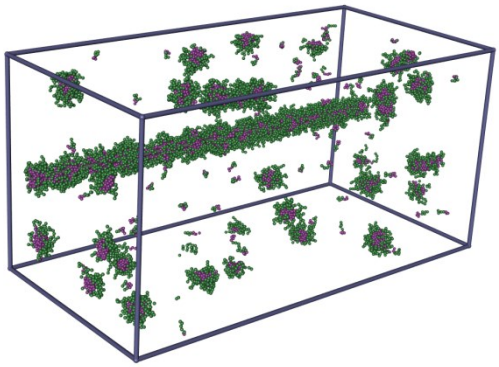

***Figure 1.*** Simulation snapshot showing the simulation box (100σ ×100σ ×200σ) and the system above the CMC.

**Reduced Units**

When describing the simulations we use reduced quantities: lengths are given in units of the LJ length parameter σ, the energy is scaled with the well depth of the bead/bead LJ interaction ε, the temperature scale is given in terms of $\varepsilon/k_B$ and time is represented in units of $\sqrt{m\sigma^2/\varepsilon}$, where m is the mass of a bead. Concentrations are defined as molecular number densities and given in units of $1/\sigma^3$

## Results and discussion

### *Computer Simulations*

Here we study adsorption of the model surfactant $H_5T_5$ with 5 hydrophilic head beads (H) and 5 hydrophobic tail beads (T) on a SWCNT. We have determined the CMC of this model surfactant in an earlier publication[75] and at a reduced temperature of T = 0.7 found $C_{CMC} = 5.2\times10^{-5}$. We observed a rather sharp transition from $C_1 = C$ to $C_1 = \text{const.}$ at the CMC, where $C_1$ is the concentration of free surfactant molecules. This allowed us to define the CMC to be the center of the very small transition region between the two domains[75]. For the further discussion it is interesting to note that this model surfactant forms spherical micelles of approximately 41 chains in bulk solution.

### Adsorption of surfactants on single wall nanotubes

We investigate adsorption of surfactants on SWCNTs using the bulk concentration as the control parameter (Figure 2). At low concentrations, the number of adsorbed surfactant molecules increases linearly with increasing concentration (Figure 2(b)). We then observe a steep increase in the adsorbed amount around $C = 2.0\times10^{-5}$. Any further increase in the concentration leads to only a very slight increase in the number of adsorbed chains. (Observe the logarithmic concentration scale.) Thus, adsorption is nearly complete at a concentration significantly smaller than the CMC, i.e. around $C \approx 0.5\ C_{CMC}$. Evidently, the leveling off of the adsorbed amount is associated with saturating the surfaces rather than with reaching the bulk CMC as in the case of adsorption on hydrophilic surfaces (e.g.[79,80]).

The initial linear region, $C<0.6\times10^{-5}$, is consistent with adsorption of individual molecules in the Henry's law regime. The evidence for adsorption of individual molecules is provided by the respective cluster size distribution in Figure 3. The cluster size distributions are defined here as the (canonical ensemble average of the) probability mass function, i.e. the probability that an adsorbed chain belongs to a cluster of aggregation number N

$$P(N) = \left\langle \frac{N n_N}{\sum_{N=1}^{\infty} N n_N} \right\rangle \qquad (4)$$

where $n_N$ is the instantaneous number of clusters of size $N$ adsorbed on the CNT and $\langle \cdots \rangle$ denotes the canonical ensemble average. At $C= 0.51\times10^{-5}$, P(N) in Figure 3 decays steeply, thus, demonstrating that at very low surfactant concentrations adsorption is dominated by individual surfactant molecules.

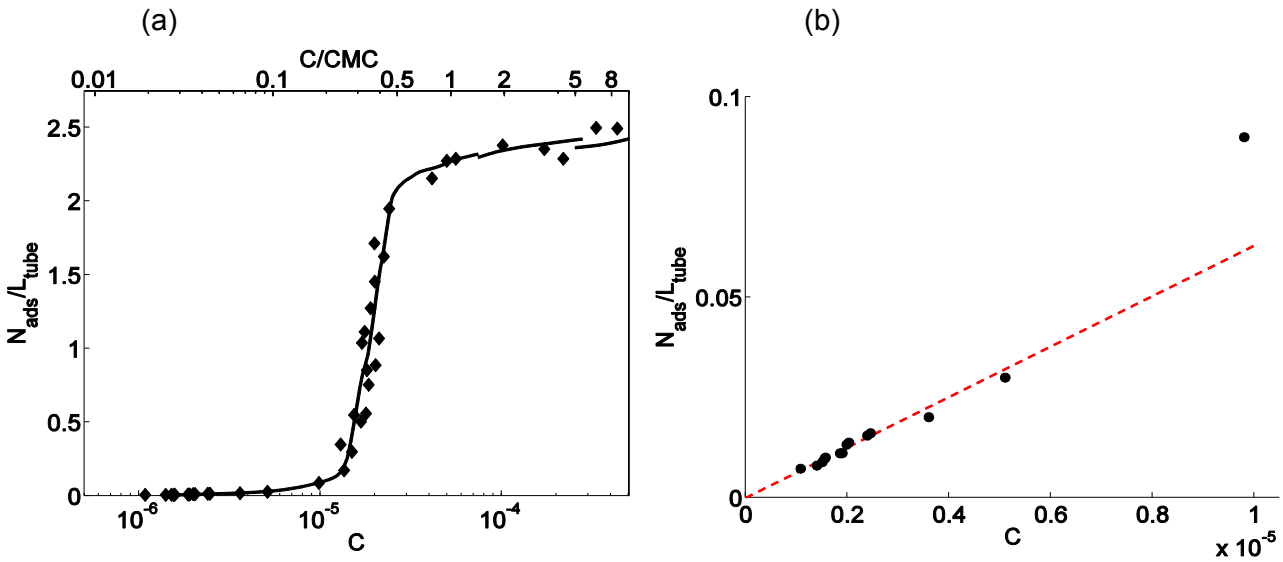


***Figure 2.*** Adsorption isotherm as number of adsorbed molecules per tube length $N_{\text{ads}} / L_{\text{tube}}$ versus bulk surfactant concentration (a) complete isotherm and (b) magnification of the low coverage regime. The solid line in part (a) is a guide to the eye and the dashed line in part (b) is a linear fit to the results for $C < 0.6 \times 10^{-5}$.

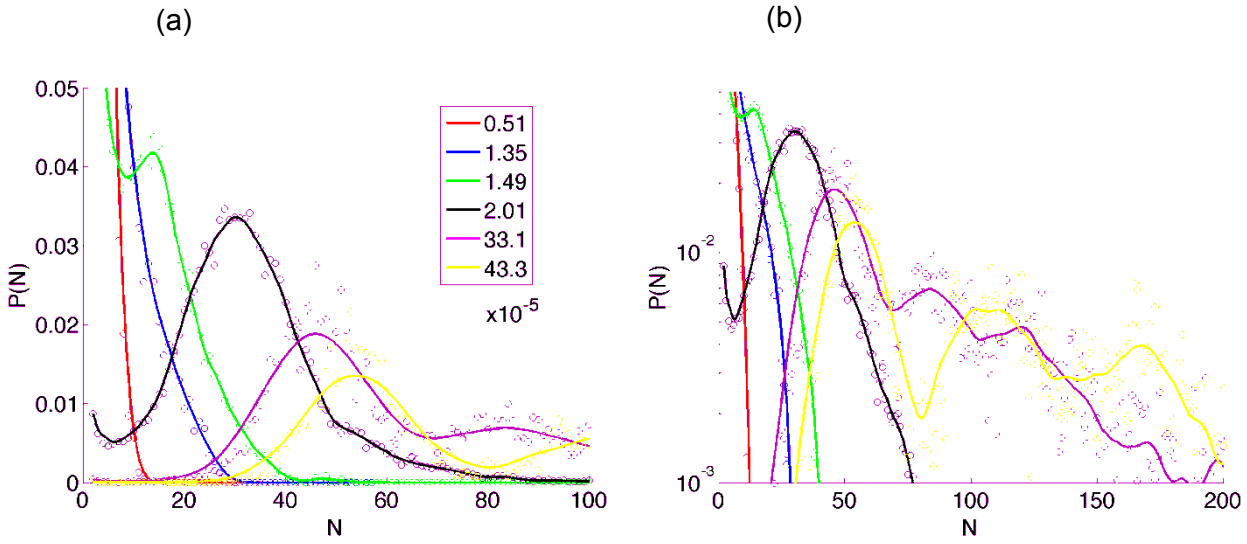


***Figure 3.*** Cluster size distributions at 6 different concentrations as indicated in part (a): (a) linear N scale and (b) logarithmic N scale to emphasize the tails at large concentrations.

As the bulk concentration increases, the adsorbed amount increases faster than linear. This superlinear increase is a clear sign of cooperative adsorption. At these still low concentrations cluster size distributions

(P(N) for C= $1.35\times10^{-5}$ in Figure 3) still decay exponentially indicating the formation of (small) clusters of no preferred size (Figure 4 (a)). Clusters in this regime form statistically and thus, grow in size with increasing concentration.

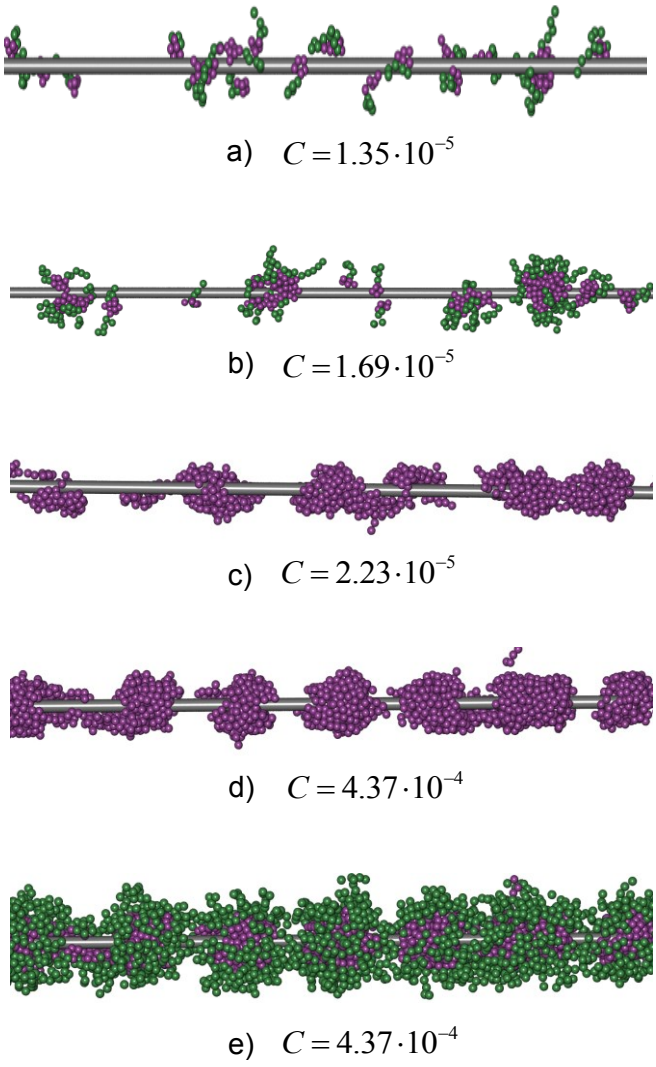


***Figure 4.*** Simulation snapshots at different bulk concentrations as indicated in the figure. In parts (a), (b), (e) the hydrophilic surfactant head beads are shown in green and the hydrophobic tail beads in purple, while in (c), (d) only the hydrophobic tail beads are shown for clarity.

As the concentration increases above a certain threshold, a shoulder appears in P(N) (Figure 3, C = $1.49\times10^{-5}$). This shoulder is indicative of the formation of clusters of preferred size, that is, surfactant aggregation on the CNT. These adsorbed aggregates are clearly visible in the snapshot in Figure 4(b). At even higher concentrations, the shoulder has developed into a well defined local maximum (Figure 3, C =

$2.39\times10^{-5}$). This indicates that adsorption is now dominated by adsorbed micelles (Figure 4(c)-(e)). The concentration where this maximum first appears is often used as a reference point for surface aggregation called Critical Surface Aggregation Concentration (CSAC). In the present case $C_{CSAC} \approx 1.5\times10^{-5} \approx 0.3\ C_{CMC}$. This surface aggregation causes the adsorbed amount to increases steeply and faster than in the initial linear regime (Figure 2). Thus, surface aggregation dominates surfactant adsorption on the small diameter tube studied here.

At concentrations immediately above the CSAC, aggregates have a size of about 13 surfactant molecules. This is significantly smaller than the aggregation number of bulk micelles which is approximately 41. As the bulk concentration increases, the aggregate size increases up to approximately 45 at $C = 33.1\times10^{-5}$. Moreover, at concentrations beyond $C \approx 2\times10^{-5}$ cluster size distributions have a tail at large cluster sizes which is caused by temporary connection of two or more clusters. This tail grows with increasing concentration. At the highest concentrations the tail has maxima at integer multiples of the position of the first peak implying the connection of two or more adsorbed micelles (Figure 4(c), (d)).

A final remark on the relevance of the simulation results for the interpretation of the experimental measurements is in place. It must be expected that the adsorbed self-assembled structures depend on the diameter of the CNTs [67,81]. Clearly, if the tube diameter is very large adsorption of concentric micelles, as shown in Figures 4(d) and (e) is not possible. Although very little is known about this, the tube diameter is likely to have influences on the adsorption isotherm.

However, in the experiments we are using single-wall CNTs where the overwhelming majority of tubes has diameters between 0.7 and 1.4 nm [82]. Typical bulk micelles of the two surfactants used in this study SDS and SDBS have diameters of ~4nm [83] and ~6nm [84], respectively. Thus, the diameters of the SWCNTs in the sample are significantly smaller than the diameter of the (bulk) micelles. This situation is well reproduced by our model where the tube diameter is 2 and the diameter of the hydrophobic core of the micelles is ~4.6 [75]. Therefore, it appears reasonable to assume that adsorption in the experimental system results in structures which are similar to the once we fine in the model system. Consequently, it is also reasonable to make qualitative comparison between the model and the experimental system.

**Stabilization of CNT suspensions by surfactants**

Steric repulsion between the head groups of surfactant molecules adsorbed onto different tubes generates a barrier against CNT rebundling. The strength of this repulsion between the coated tubes depends on many parameters such as the strength of the repulsive interaction between the head groups, the distance dependence of this interaction, the flexibility of the head groups, the temperature etc. However, it is reasonable to assume that the shielding against rebundling is better the higher the density of the head groups is.

This is difficult to assess from snapshots such as the one shown in Figure 4(e). However, together with Figure 4(d) it shows that although surfactant molecules form adsorbed micelles and thus generate a very heterogeneous structure of adsorbed surfactant tails, surfactant head groups are much more evenly distributed. Therefore, it is sensible to introduce a radial density profile which is defined as the (canonical ensemble average of the) local density of head beads at distance R from the tube axis averaged over the length of the tube and rotation around the tube axis. These density profiles are shown in Figure 5.

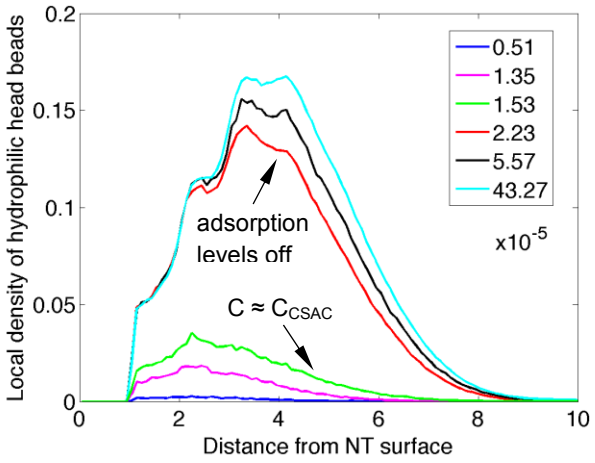


***Figure 5.*** Radial density distributions of head groups as the local density of heads groups as a function of distance from the tube surface at various concentrations indicated in the figure. Head densities are low below the CSAC, increase quickly just after the CSAC and remain essentially unchanged when the adsorbed amount levels off at $C \approx 2\times10^{-5}$.

In the lower concentration regime, i.e. for values below the CSAC the density of head-groups is low and increases only slightly with increasing concentration. As the concentration increases past the CSAC, the head density quickly increases. This is consistent with the steep increase of the adsorbed amount at the CSAC. As discussed above, adsorption is essentially complete at $C \approx 2\times10^{-5}$. Consequently, the head density remains almost constant if the concentration is increased beyond $C \approx 2\times10^{-5}$. As the density profiles do not show significant changes after the leveling-off of the adsorbed amount somewhat above the CSAC, we do not expect significantly improved shielding for surfactant concentrations well beyond the CSAC. In other words, our results indicate that a concentration just above the CSAC, and thus significantly lower than the CMC, should be sufficient to stabilize the dispersion. If this is insufficient for stabilization, any further concentration increase should not improve the stabilization significantly.

***Experimental results***

In order to verify the predictions of the simulations we prepared a series of dispersions of SWCNTs in solutions of the anionic surfactants SDS and SDBS for a wide range of concentrations above and below the CMC.

After centrifugation of the original dispersions, the resultant supernatant fractions had different color densities. For the SDS series the color density clearly decreased with decreasing surfactant concentration, while for the SDBS series only sample SDBS02 (C=0.53 $C_{CMC}$) appeared less dense than dispersions obtained with surfactant concentrations above the CMC. The actual SWCNT concentrations in dispersions were determined by means of Raman spectroscopy.[85] The original dispersions SDS10 and SDBS3 with concentration ($c_0$) of 0.1 mg SWCNT per ml were diluted with appropriate surfactant to a series of concentrations ($c/c_0$ of 0.75, 0.5 and 0.25) immediately after ultrasonic treatment. These dispersions with known concentrations were then used for creation of the plot of concentration vs. $G^+$-peak area normalized to the water peak ($\nu_{O-H}$) [85]. The resulting calibration curve was then used for determination of concentrations in dispersions after centrifugation (Figure 6). The concentration values for the centrifuged dispersions are shown in Table 2.

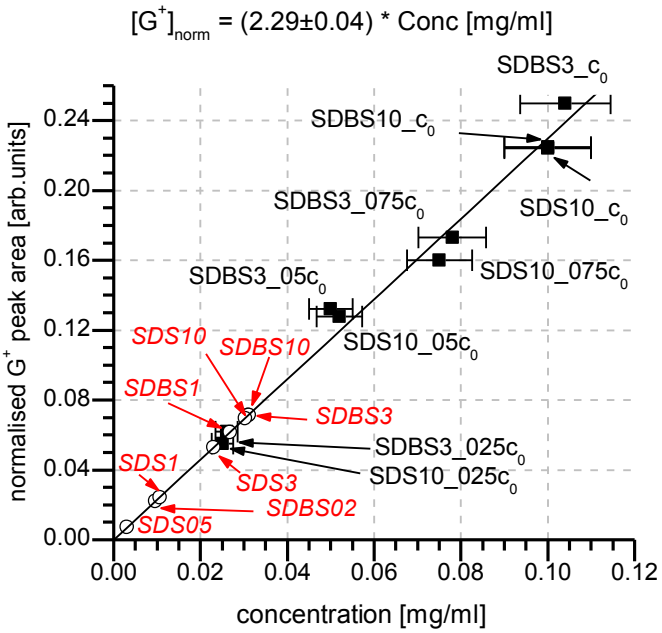


***Figure 6.*** $G^+$-band area normalized to water peak ($\nu_{O-H}$) versus concentration. Dispersions with known concentrations are marked with black squares and were used for creating the linear concentration calibration curve. The unknown concentrations for dispersions after centrifugation (small circles) were estimated on the basis of the normalized area of the $G^+$-band in the Raman spectra of corresponding dispersions and the created calibration line.

The diameter distributions of both individual SWCNT and nanotube bundles in the obtained dispersions for different surfactants after centrifugation were measured by AFM. In order to obtain sufficient statistics, about 200 species were measured for each dispersion sample. We assume that the process of 'sticking' of the SWCNT from dispersion to the functionalized Si surface under normal gravity and after centrifugation is random and governed only by the Brownian motion of tubes in solution. Therefore, the diameter distribution of tubes/bundles obtained from AFM height measurements should directly represent the aggregation state of the SWCNT in dispersion. In our SWCNT samples the diameter (i.e. the AFM profile height) distributions for all concentrations of surfactants fitted well with LogNormal distributions, however, with different widths and positions of maximum, as shown in Figures 7 and 8.

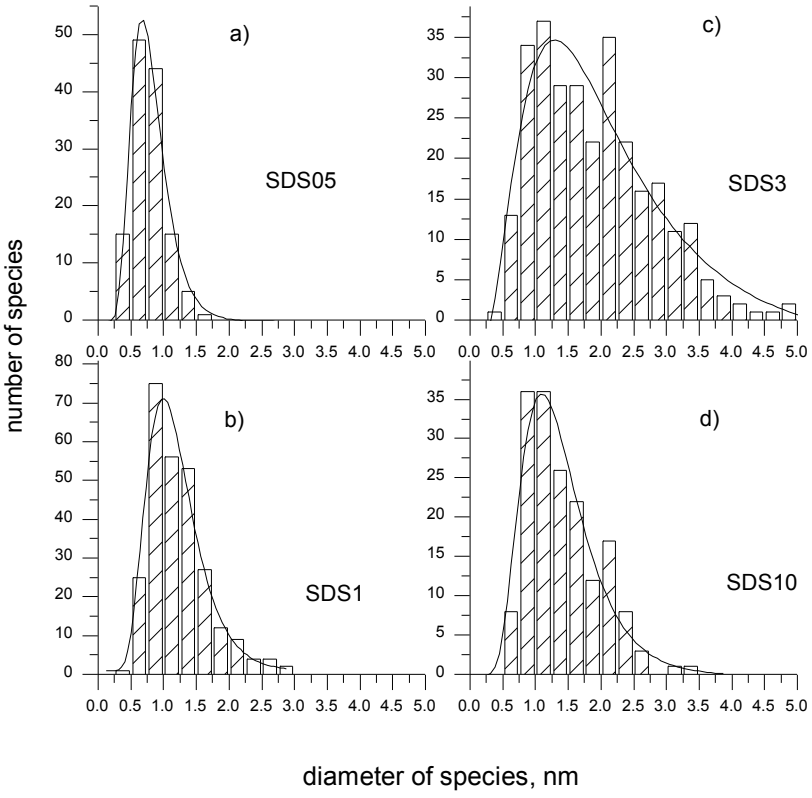


***Figure 7.*** Diameter distribution of SWCNT species in centrifuged SDS dispersions prepared at different surfactant concentrations: a) 0.5 mg SDS /ml of solution, b) 1 mg SDS /ml, c) 3 mg SDS /ml and d) 10 mg SDS/ml.

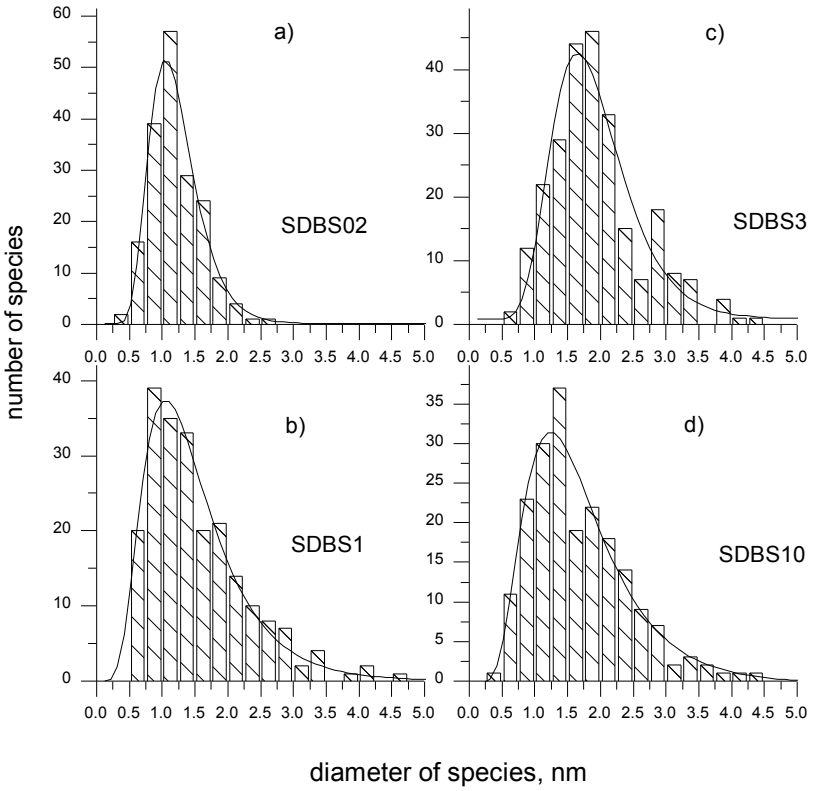


***Figure 8.*** Diameter distribution of SWCNT species in centrifuged SDBS dispersions prepared at different surfactant concentrations: a) 0.2 mg SDBS /ml of solution, b) 1 mg SDBS /ml, c) 3 mg SDBS /ml and d) 10 mg SDBS /ml.

The AFM data (Figures 7 and 8) clearly exhibit a decrease in diameter values in dispersions with surfactant concentrations below the CMC as follows from a shift of distribution maxima and its narrowing towards lower numbers. Additionally, the root-mean-square of the diameter distribution ($D_{rms} = (\sqrt{<D^2>})$ of tubes in dispersion, previously used by Coleman et al. [41,42,59,86-88] for estimation of the fraction of individual tubes per volume, also shows a significant decrease for dispersions produced in surfactant solutions below the CMC (Table 2). The difference in experimental conditions during preparation of dispersions (centrifugation carried out at 3000×g by Sun et al [59] and 20000×g in our case) resulted in our dispersions showing $D_{rms}$ values <2 (and even <1 for the solution SDS05), contrary to Sun's data [59] where $D_{rms}$ stabilized at values of ~2.4 nm. Although still significant, the mass fraction (concentration) of SWCNT in surfactant solutions below CMC is lower than in solutions above CMC, in general correspondence with literature data [59]. It is interesting to note that the w/w ratio of surfactant-to-SWCNT shows the tendency to decrease along with the decrease of the surfactant concentration (Table 2).

The HiPco individual SWCNT have diameters in the range 0.7 – 1.4 nm [82,89]. Simple geometry considerations show that an AFM height profile of 1.3 nm may be the result of a bundle consisting of three tubes with diameter of 0.7 nm. Bundles composed of thicker tubes and/or greater number of tubes should have larger diameters. Therefore in further analysis of dispersions we assume that the species with heights < 1.3 nm are individual carbon nanotubes. (This could also include agglomerates of two carbon nanotubes lying flat on the substrate surface). Thus, from AFM based height distributions it follows that for dispersions SDBS02 and SDS1 (0.53 CMC and 0.43 CMC respectively) the content of individual tubes in dispersion is around 65% at a fairly high concentration of tubes of approximately 0.01 mg/ml. The dispersion SDS05 (~0.2 CMC) consists practically completely of individual tubes (98%) with a CNT concentration of $3*10^{-3}$ mg/ml. The SWCNT dispersions prepared from surfactant solutions above CMC exhibit an individual tube content of only 22 - 52% (Table 2).

Additional information on the bundle size distribution in SWCNT dispersions below CMC may be extracted from the maximum diameter value of deposited species. It is obvious from diameter distributions in our samples (Figures 7 and 8) that centrifugation of dispersions at 20000×g completely removes the species with diameters >5nm. If it is assumed that the sedimentation velocity of SWCNT aggregates in surfactant solution depends on the number of tubes in the bundle (i.e. bundle size)[90], then all examined dispersions should contain species with diameters of no more than 5 nm. Indeed, a significant amount of species with diameters $3.5<d_t<5$ nm is observed for all dispersions with surfactant concentration above CMC, except for SDS10 with a maximum diameter value of 3.3 nm (Table 2). It is, however, interesting that for SWCNT dispersions, prepared in below-CMC surfactant solutions, the maximum diameter values are 2.8 nm for SDS1, 2.25 nm for SDBS02 and 1.5 nm for SDS05 dispersions. Thus, only small aggregates are stabilized in dispersions with surfactant solutions below the CMC. There are two possible explanations for this: (i) surfactant adsorption is insufficient to prevent the reagglomeration of small to larger bundles or (ii) it is insufficient to stabilize the small bundles in the suspension against the centrifugal force. In any case, our results suggest that adsorption on individual tubes and bundles might follow different surfactant concentration dependencies and possibly different mechanisms.

**Summary and Conclusions**

In this manuscript we present the results of an experimental/theoretical study of the physical processes relevant to the dispersion of CNTs. In particular we have investigated the dispersive capabilities of surfactant solutions below the CMC.

The experiments were carried out on HiPco SWCNTs with two surfactants SDS and SDBS, with different CMC values $C_{CMC}(SDS) \approx 6\ C_{CMC}(SDBS)$. The results obtained for both surfactants are remarkably similar if the concentration scale is normalized by the respective CMC. In both systems we find:

1) CNT may be dispersed in surfactant solutions below the CMC.

2) A relatively small but significant fraction of tubes is suspended in below-CMC dispersions.

3) SWCNT in surfactant solutions below CMC show a tendency to be dispersed as individual tubes and small bundles.

4) Diameter distribution of SWCNT species in above-CMC surfactant dispersions is significantly broader and is shifted to larger diameters, compared to in below-CMC dispersions.

Using computer simulations of a coarse-grained model we studied the concentration dependence of surfactant adsorption on a small individual SWCNT. The simulation results show:

1) Adsorption is essentially complete at approximately 0.5 CMC.

2) Above the CMC only minimal changes in the adsorbed amount and the radial head density profile are observed.

3) Adsorption is dominated by surfactant self-assembly.

To develop an understanding of the experimentally obtained diameter distributions it is important to realize that the experimental results are influenced by three processes: (i) ultrasonication, (ii) relaxation to equilibrium and (iii) centrifugation. The latter, centrifugation, is also the last processing step before the samples are measured and might, therefore, dominate the results.

Centrifugation separates objects with higher density (larger agglomerates of SWCNT) out of solution. In the present case these objects are CNT/surfactant composites. Although it is difficult to determine the boundaries of these CNT/surfactant composites as they are soft and have attractive interactions with water, it is clear that a higher number of adsorbed surfactant molecules reduces the over all density of the complex and makes them more hydrophilic. Both effects support the dispersibility of the CNT/surfactant composite.

The simulation results show that surfactant adsorption on small tubes is essentially complete well below the CMC. This means that increasing the concentration beyond the CMC should not further improve the dispersibility of individual CNTs. This is consistent with our experimental observation of dispersed individual tubes below the CMC.

There remain a number of key questions that need further clarification:

1) Why are small bundles dispersed only at higher concentration? This indicates a different adsorption mechanism compared to individual tubes which might be caused by the different surface morphologies and interaction energies of bundles compared to individual tubes.

2) Why does the number of dispersed individual tubes increase with concentration? This can only happen if the number of exfoliated tubes depends on the concentration.

3) What is the actual surfactant concentration in the sample? Surfactant adsorption on all available surfaces, including CNTs as well as the containers, decreases the number of molecules in solution and thus the concentration. However, for detailed interpretation and comparability of the experimental results knowledge of the actual concentration is essential.

Further experimental and simulation studies are in progress to provide answers.

**References**


[1] Coleman, J. N.; Khan, U.; Gun'ko, Y. K. *Advanced Materials* **2006**, *18*, 689.

[2] Thostenson, E. T.; Chou, T.-W. *Journal of Physics D: Applied Physics* **2002**, L77.

[3] Reibold, M.; Paufler, P.; Levin, A. A.; Kochmann, W.; Patzke, N.; Meyer, D. C. *Nature* **2006**, *444*, 286.

[4] Regev, O.; ElKati, P. N. B.; Loos, J.; Koning, C. E. *Advanced Materials* **2004**, *16*, 248.

[5] Suryasarathi, B.; Arup, R. B.; Rupesh, A. K.; Ajit, R. K.; Patro, T. U.; Sivaraman, P. *Nanotechnology* **2008**, 335704.

[6] Star, A.; Stoddart, J. F.; Steuerman, D.; Diehl, M.; Boukai, A.; Wong, E. W.; Yang, X.; Chung, S.-W.; Choi, H.; Heath, J. R. *Angewandte Chemie International Edition* **2001**, *40*, 1721.

[7] Yamamoto, T.; Watanabe, K.; Hernández, E. Mechanical Properties, Thermal Stability and Heat Transport in Carbon Nanotubes. In *Topics in Applied Physics: Carbon Nanotubes*; Springer Berlin / Heidelberg, 2008; pp 165.

[8] Hsu, I. K.; Pettes, M. T.; Bushmaker, A.; Aykol, M.; Shi, L.; Cronin, S. B. *Nano Letters* **2009**, *9*, 590.

[9] Yu, A.; Ramesh, P.; Sun, X.; Bekyarova, E.; Itkis, M. E.; Haddon, R. C. *Advanced Materials* **2008**, *20*, 4740.

[10] Wang, S.; Liang, R.; Wang, B.; Zhang, C. *Carbon* **2009**, *47*, 53.

[11] Duong, H. M.; Papavassiliou, D. V.; Mullen, K. J.; Wardle, B. L.; Maruyama, S. *The Journal of Physical Chemistry C* **2008**, *112*, 19860.

[12] Cai, D.; Song, M. *Carbon* **2008**, *46*, 2107.

[13] Arnold, M. S.; Green, A. A.; Hulvat, J. F.; Stupp, S. I.; Hersam, M. C. *Nature Nanotechnology* **2006**, *1*, 60.

[14] Tu, X.; Zheng, M. *Nano Research* **2008**, *1*, 185.

[15] Lopez-Pastor, M.; Dominguez-Vidal, A.; Ayora-Canada, M. J.; Simonet, B. M.; Lendl, B.; Valcarcel, M. *Analytical Chemistry* **2008**, *80*, 2672.

[16] Arnold, M. S.; Stupp, S. I.; Hersam, M. C. *Nano Letters* **2005**, *5*, 713.

[17] Green, A. A.; Hersam, M. C. *Nano Letters* **2008**, *8*, 1417.

[18] Zheng, M.; Jagota, A.; Strano, M. S.; Santos, A. P.; Barone, P.; Chou, S. G.; Diner, B. A.; Dresselhaus, M. S.; McLean, R. S.; Onoa, G. B.; Samsonidze, G. G.; Semke, E. D.; Usrey, M.; Walls, D. J. *Science* **2003**, *302*, 1545.

[19] Strano, M. S.; Moore, V. C.; Miller, M. K.; Allen, M. J.; Haroz, E. H.; Kittrell, C.; Hauge, R. H.; Smalley, R. E. *Journal of Nanoscience and Nanotechnology* **2003**, *3*, 81.

[20] Vaisman, L.; Wagner, H. D.; Marom, G. *Advances in Colloid and Interface Science* **2006**, *128-130*, 37.

[21] Gong, X.; Liu, J.; Baskaran, S.; Voise, R. D.; Young, J. S. *Chemistry of Materials* **2000**, *12*, 1049.

[22] Islam, M. F.; Rojas, E.; Bergey, D. M.; Johnson, A. T.; Yodh, A. G. *Nano Letters* **2003**, *3*, 269.

[23] Wenseleers, W.; Vlasov, I. I.; Goovaerts, E.; Obraztsova, E. D.; Lobach, A. S.; Bouwen, A. *Advanced Functional Materials* **2004**, *14*, 1105.

[24] Fugetsu, B.; Han, W.; Endo, N.; Kamiya, Y.; Okuhara, T. *Chemistry Letters* **2005**, *34*, 1218.

[25] O'Connell, M. J.; Boul, P.; Ericson, L. M.; Huffman, C.; Wang, Y.; Haroz, E.; Kuper, C.; Tour, J.; Ausman, K. D.; Smalley, R. E. *Chemical Physics Letters* **2001**, *342*, 265.

[26] Manivannan, S.; Jeong, I.; Ryu, J.; Lee, C.; Kim, K.; Jang, J.; Park, K. *Journal of Materials Science: Materials in Electronics* **2009**, *20*, 223.

[27] Tetsuya Uchida, S. K. *Journal of Applied Polymer Science* **2005**, *98*, 985.

[28] Rasheed, A.; Dadmun, M. D.; Ivanov, I.; Britt, P. F.; Geohegan, D. B. *Chemistry of Materials* **2006**, *18*, 3513.

[29] Rice, N. A.; Soper, K.; Zhou, N.; Merschrod, E.; Zhao, Y. *Chemical Communications* **2006**, 4937.

[30] Chen, H.; Xue, Q.; Zheng, Q.; Xie, J.; Yan, K. *The Journal of Physical Chemistry C* **2008**, *112*, 16514.

[31] Ortiz-Acevedo, A.; Xie, H.; Zorbas, V.; Sampson, W. M.; Dalton, A. B.; Baughman, R. H.; Draper, R. K.; Musselman, I. H.; Dieckmann, G. R. *Journal of the American Chemical Society* **2005**, *127*, 9512.

[32] Zheng, M.; Jagota, A.; Semke, E. D.; Diner, B. A.; McLean, R. S.; Lustig, S. R.; Richardson, R. E.; Tassi, N. G. *Nature Materials* **2003**, *2*, 338.

[33] Salzmann, C. G.; Lee, G. K. C.; Ward, M. A. H.; Chu, B. T. T.; Green, M. L. H. *Journal of Materials Chemistry* **2008**, *18*, 1977.

[34] Takahashi, T.; Tsunoda, K.; Yajima, H.; Ishii, T. *Japanese Journal of Applied Physics, Part 1: Regular Papers, Short Notes & Review Papers* **2004**, *43*, 3636.

[35] Minami, N.; Kim, Y.; Miyashita, K.; Kazaoui, S.; Nalini, B. *Applied Physics Letters* **2006**, *88*, 093123/1.

[36] Yan, L. Y.; Poon, Y. F.; Chan-Park, M. B.; Chen, Y.; Zhang, Q. *The Journal of Physical Chemistry C* **2008**, *112*, 7579

[37] Star, A.; Steuerman, D. W.; Heath, J. R.; Stoddart, J. F. *Angewandte Chemie International Edition* **2002**, *41*, 2508.

[38] Fukushima, T.; Kosaka, A.; Ishimura, Y.; Yamamoto, T.; Takigawa, T.; Ishii, N.; Aida, T. *Science* **2003**, *300*, 2072.

[39] Wang, J.; Li, Y. *Journal of the American Chemical Society* **2009**, *131*, 5364.

[40] Wang, J.; Chu, H.; Li, Y. *ACS Nano* **2008**, *2*, 2540.

[41] Giordani, S.; Bergin, S. D.; Nicolosi, V.; Lebedkin, S.; Kappes, M. M.; Blau, W. J.; Coleman, J. N. *The Journal of Physical Chemistry B* **2006**, *110*, 15708.

[42] Bergin, S. D.; Nicolosi, V.; Giordani, S.; de Gromard, A.; Carpenter, L.; Blau, W. J.; Coleman, J. N. *Nanotechnology* **2007**, *18*, 455705.

[43] Banerjee, S.; Hemraj-Benny, T.; Wong, S. S. *Advanced Materials* **2005**, *17*, 17.

[44] Hilding, J.; Grulke, E. A.; Zhang, Z. G.; Lockwood, F. *Journal of Dispersion Science and Technology* **2003**, *24*, 1

[45] Penicaud, A.; Poulin, P.; Derre, A.; Anglaret, E.; Petit, P. *Journal of the American Chemical Society* **2005**, *127*, 8.

[46] Price, B. K.; Tour, J. M. *Journal of the American Chemical Society* **2006**, *128*, 12899.

[47] Wang, Y.; Iqbal, Z.; Mitra, S. *Journal of the American Chemical Society* **2006**, *128*, 95.

[48] Bauer, B. J.; Becker, M. L.; Bajpai, V.; Fagan, J. A.; Hobbie, E. K.; Migler, K.; Guttman, C. M.; Blair, W. R. *The Journal of Physical Chemistry C* **2007**, *111*, 17914.

[49] Hung, N.; Anoshkin, I.; Dementjev, A.; Katorov, D.; Rakov, E. *Inorganic Materials* **2008**, *44*, 219.

[50] Kharisov, B. I.; Kharissova, O. V.; Gutierrez, H. L.; Mendez, U. O. *Industrial & Engineering Chemistry Research* **2009**, *48*, 572.

[51] Zhao, J.; Park, H.; Han, J.; Lu, J. P. *The Journal of Physical Chemistry B* **2004**, *108*, 4227.

[52] Umeyama, T.; Tezuka, N.; Fujita, M.; Matano, Y.; Takeda, N.; Murakoshi, K.; Yoshida, K.; Isoda, S.; Imahori, H. *The Journal of Physical Chemistry C* **2007**, *111*, 9734.

[53] Fagan, S. B.; da Silva, A. J. R.; Mota, R.; Baierle, R. J.; Fazzio, A. *Physical Review B* **2003**, *67*, 033405.

[54] Lu, J.; Wang, D.; Nagase, S.; Ni, M.; Zhang, X.; Maeda, Y.; Wakahara, T.; Nakahodo, T.; Tsuchiya, T.; Akasaka, T.; Gao, Z.; Yu, D.; Ye, H.; Zhou, Y.; Mei, W. N. *The Journal of Physical Chemistry B* **2006**, *110*, 5655.

[55] Cho, E.; Kim, H.; Kim, C.; Han, S. *Chemical Physics Letters* **2006**, *419*, 134.

[56] Kang, H. S. *The Journal of Chemical Physics* **2004**, *121*, 6967.

[57] Kim, K. S.; Bae, D. J.; Kim, J. R.; Park, K. A.; Lim, S. C.; Kim, J. J.; Choi, W. B.; Park, C. Y.; Lee, Y. H. *Advanced Materials* **2002**, *14*, 1818.

[58] Bonard, J.-M.; Stora, T.; Salvetat, J.-P.; Maier, F.; Stöckli, T.; Duschl, C.; Forró, L.; de Heer, W. A.; Châtelain, A. *Advanced Materials* **1997**, *9*, 827.

[59] Sun, Z.; Nicolosi, V.; Rickard, D.; Bergin, S. D.; Aherne, D.; Coleman, J. N. *The Journal of Physical Chemistry C* **2008**, *112*, 10692.

[60] Utsumi, S.; Kanamaru, M.; Honda, H.; Kanoh, H.; Tanaka, H.; Ohkubo, T.; Sakai, H.; Abe, M.; Kaneko, K. *Journal of Colloid and Interface Science* **2007**, *308*, 276.

[61] Moore, V. C.; Strano, M. S.; Haroz, E. H.; Hauge, R. H.; Smalley, R. E.; Schmidt, J.; Talmon, Y. *Nano Letters* **2003**, *3*, 1379.

[62] Matarredona, O.; Rhoads, H.; Li, Z.; Harwell, J. H.; Balzano, L.; Resasco, D. E. *The Journal of Physical Chemistry B* **2003**, *107*, 13357.

[63] McDonald, T. J.; Engtrakul, C.; Jones, M.; Rumbles, G.; Heben, M. J. *The Journal of Physical Chemistry B* **2006**, *110*, 25339.

[64] Nativ-Roth, E.; Shvartzman-Cohen, R.; Bounioux, C.; Florent, M.; Zhang, D.; Szleifer, I.; Yerushalmi-Rozen, R. *Macromolecules* **2007**, *40*, 3676.

[65] Wallace, E. J.; Mark, S. P. S. *Nanotechnology* **2009**, 045101.

[66] Wallace, E. J.; Sansom, M. S. P. *Nano Letters* **2007**, *7*, 1923.

[67] Tummala, N. R.; Striolo, A. *ACS Nano* **2009**, *3*, 595.

[68] Patel, N.; Egorov, S. A. *Journal of the American Chemical Society* **2005**, *127*, 14124.

[69] Nikolaev, P.; Bronikowski, M. J.; Bradley, R. K.; Rohmund, F.; Colbert, D. T.; Smith, K. A.; Smalley, R. E. *Chemical Physics Letters* **1999**, *313*, 91.

[70] Mukerjee, P.; Kapauan, P.; Meyer, H. G. *The Journal of Physical Chemistry* **1966**, *70*, 783.

[71] Thévenot, C.; Grassl, B.; Bastiat, G.; Binana, W. *Colloids and Surfaces A: Physicochemical and Engineering Aspects* **2005**, *252*, 105.

[72] Liu, J.; Casavant, M. J.; Cox, M.; Walters, D. A.; Boul, P.; Lu, W.; Rimberg, A. J.; Smith, K. A.; Colbert, D. T.; Smalley, R. E. *Chemical Physics Letters* **1999**, *303*, 125.

[73] Lewenstein, J. C.; Burgin, T. P.; Ribayrol, A.; Nagahara, L. A.; Tsui, R. K. *Nano Letters* **2002**, *2*, 443.

[74] Burgin, T. P.; Lewenstein, J. C.; Werho, D. *Langmuir* **2005**, *21*, 6596.

[75] Angelikopoulos, P.; Bock, H. *The Journal of Physical Chemistry B* **2008**, *112*, 13793.

[76] Weisstein, E. W. Point-Line Distance--3-Dimensional. In *MathWorld--A Wolfram Web Resource*.

[77] Robert, D. G.; Patrick, B. W. *The Journal of Chemical Physics* **1997**, *107*, 4423.

[78] Rekvig, L.; Kranenburg, M.; Vreede, J.; Hafskjold, B.; Smit, B. *Langmuir* **2003**, *19*, 8195.

[79] Bock, H.; Gubbins, K. E. *Physical Review Letters* **2004**, *92*, 135701.

[80] Dietsch, O.; Eltekov, A.; Bock, H.; Gubbins, K. E.; Findenegg, G. H. *The Journal of Physical Chemistry C* **2007**, *111*, 16045.

[81] Richard, C.; Balavoine, F.; Schultz, P.; Ebbesen, T. W.; Mioskowski, C. *Science* **2003**, *300*, 775.

[82] Brar, V. W.; Samsonidze, G. G.; Santos, A. P.; Chou, S. G.; Chattopadhyay, D.; Kim, S. N.; Papadimitrakopoulos, F.; Zheng, M.; Jagota, A.; Onoa, G. B.; Swan, A. K.; Unlu M.S; Goldberg, B. B.; Dresselhaus, G.; Dresselhaus, M. S. *Journal of Nanoscience and Nanotechnology* **2005**, *5*, 209.

[83] Hassan, P. A.; Fritz, G.; Kaler, E. W. *Journal of Colloid and Interface Science* **2003**, *257*, 154.

[84] Segota, S.; Heimer, S.; Tezak, Đ. *Colloids and Surfaces A: Physicochemical and Engineering Aspects* **2006**, *274*, 91.

[85] Salzmann, C. G.; Chu, B. T. T.; Tobias, G.; Llewellyn, S. A.; Green, M. L. H. *Carbon* **2007**, *45*, 907.

[86] Cathcart, H.; Quinn, S.; Nicolosi, V.; Kelly, J. M.; Blau, W. J.; Coleman, J. N. *The Journal of Physical Chemistry C* **2007**, *111*, 66.

[87] Bergin, S. D.; Nicolosi, V.; Cathcart, H.; Lotya, M.; Rickard, D.; Sun, Z.; Blau, W. J.; Coleman, J. N. *The Journal of Physical Chemistry C* **2008**, *112*, 972.

[88] Bergin, S. D.; Nicolosi, V.; Streich, P. V.; Giordani, S.; Sun, Z.; Windle, A. H.; Ryan, P.; Niraj, N. P. P.; Wang, Z.-T. T.; Carpenter, L.; Blau, W. J.; Boland, J. J.; Hamilton, J. P.; Coleman, J. N. *Advanced Materials* **2008**, *20*, 1876.

[89] Izard, N.; Riehl, D.; Anglaret, E. *Los Alamos National Laboratory, Preprint Archive, Condensed Matter* **2005**, 1; http://arxiv1.library.cornell.edu/abs/cond-mat/0501426.

[90] Nadler, M.; Mahrholz, T.; Riedel, U.; Schilde, C.; Kwade, A. *Carbon* **2008**, *46*, 1384.